Available online at www.sciencedirect.com
ScienceDirect
Chemie der Erde 66 (2006) 307–314
CHEMIE der ERDE GEOCHEMISTRY
www.elsevier.de/chemer

Compositional variation in Hg-bearing sphalerite from the polymetallic Eskay Creek deposit, British Columbia, Canada

Tassos A. Grammatikopoulos[a,*], Oleg Valeyev[b], Tina Roth[c]

[a]*Department of Geology, Section of Earth Materials, University of Patras, GR- 26504 Patras, Greece*
[b]*SGS Lakefield Research Limited, 185 Concession Street, PO 4300 Lakefield, Ontario, Canada K0L 2H0*
[c]*Barrick Gold Corporation, Eskay Creek Mine, P.O. Box 3908, Smithers, B.C., Canada V0J 2N0*

Received 5 July 2005; accepted 16 September 2005

Abstract

The Eskay Creek, British Columbia, Canada, is a polymetallic, gold- and silver-rich, volcanic-hosted, massive sulfide deposit. The ore in the deposit is divided into subzones distinguished by mineralogy, texture, grade and metallurgical characteristics. This study presents the results of a mineralogical examination of three composite field samples, with emphasis on the chemistry of sphalerite. Sphalerite is associated with variable amounts of Hg-tetrahedrite and cinnabar, and an array of sulfides, sulphosalts and non-opaque minerals. Electron micro probe analyses of sphalerite in the three composite samples reveal wide variations in compositions. The Hg content in sphalerite in the three samples varies between 0.08 and 16.35 wt%, whereas the Fe content ranges from 0.33 to 2.29 wt%. The chemical formula of the sphalerite shows the compositional range $(Zn_{0.89–0.98}Hg_{0.01–0.09.}Fe_{0.005–0.02})S$. Sphalerite exhibits an almost perfect substitution of Hg and Zn, as shown by the negative covariance between them. Sphalerite with the highest Hg contents tends to have the lowest Fe concentrations. The highest Hg contents in sphalerite are recorded in the samples with the highest bulk Hg concentrations and with the highest cinnabar contents.

The compositional variations of sphalerite are important because they can be used in mapping ore forming fluids and indicate possible temporal variations. Second, determination of the compositional variation of the sphalerite in the mine has metallurgical implications because the mineral is an important Zn source. The mineralogical data indicate that non-physical processes (e.g. pyrometallurgy) must be used to separate Hg from Zn concentrates, with direct environmental implications, that is, release of metals, such as Hg, into the environment during mining and processing.

Keywords: Eskay Creek; Hg-rich sphalerite; Mineralogy

1. Introduction

A mineralogical examination has been carried out on three composite samples from a localized Hg-rich part in the Eskay Creek Deposit, British Columbia, Canada. Each of the composite samples is comprised of a number of samples, from different localities in the Hg-rich part of the deposit that were ground and blended to create the three composite samples. These were initially used for metallurgical tests. This paper describes briefly the overall mineralogy with emphasis on the nature of the Hg–Fe-bearing sphalerite, illustrates the extent of

*Corresponding author. Tel.: +30 2610 99 63 05; fax: +30 2610 99 75 60.
E-mail address: tassosg@upatras.gr (T.A. Grammatikopoulos).

0009-2819/$ - see front matter
doi:10.1016/j.chemer.2005.11.003

compositional variations in that Hg-rich part of the Eskay Creek polymetallic deposit, and provides insights into geological, metallurgical and environmental implications. Sphalerite is an important source of Zn, thus, Hg and Fe contents in the mineral are essential to determine possible differences among the composite samples, but also the degree of contamination of Zn concentrate, and possible methods of extraction (Grammatikopoulos and Roth, 2002).

2. Analytical methods

Electron micro probe analyses (EMPA) of minerals were carried out at SGS Lakefield Research Ltd., Canada, with Superprobe JEOL-733 equipped with Tracor Noran ED and four WDS spectrometers (LiF, PET, TAP and PET crystals). The EDS system was used only for a preliminary mineral identification. The analytical conditions of WDS analyses were maintained and monitored by Geller dQant software at 20 kV accelerating voltage, 30 nA cup electron beam providing the beam spot size on the specimen surface of 1–3 μm. The 30 s time was used to collect counts on the element peaks and both-side backgrounds during the calibration and mineral analyses. The detection limits of the elements were calculated based on the 3σ statistical precision approach. Concentrations of fifteen elements were determined at each point of analysis (S, Fe, Cu, Zn, Pb, Mn, Ag, Au, As, Te, Sb, Sn, Bi, Hg, and Se). However, Bi, Se, Te, As, Au and Sn were found below the 3σ detection limit of EMPA and they are not reported in this paper. The limits of detection for the reported analyzed elements are shown in Table 1. The following natural and synthetic mineral standards from CANMET and SPI Supplies were used for microprobe calibration. Synthetic pyrrhotite Cabri-241 (Fe La LiF crystal), synthetic Ag-calaverite (Te La PET crystal, Au LKa LiF crystal), synthetic $AgBiSe_2$ Cabri-499 (Ag La PET crystal, Se La TAP crystal, Bi La LiF crystal), synthetic chalcopyrite (Cu Ka LiF crystal), arsenopyrite (As La TAP crystal), synthetic galena Cabri-477 (Pb La PET crystal), stibnite (Sb La PET crystal), 99.9985% tin metal (Sn La PET crystal), cinnabar (Hg La LiF crystal), 99.99% manganese metal (Mn Ka LiF crystal), synthetic Fe-sphalerite Cabri-21 (Zn Ka LiF crystal, S Ka PET crystal). The compositions of all standards were cross-checked before and after the microprobe analyses. Special care was taken to analyze the highly volatile mercury in minerals by frequently re-calibrating and collecting Hg La by LiF crystal in the beginning of each new mineral analysis.

Table 1. Limits of detection (LOD) for elements analyzed for 30 s counting time

Element	LOD%
Ag	0.081
Cu	0.035
Fe	0.03
Hg	0.162
Mn	0.025
Pb	0.222
S	0.037
Sb	0.057
Zn	0.1

3. Geology and mineralization

The Eskay Creek deposit (Fig. 1) is located in British Columbia, Canada. It is hosted in middle Jurassic volcanic and sedimentary rocks. Starting at the base, the host sequence comprises a succession of andesite, marine sedimentary rocks, intermediate to felsic volcanoclastic rocks, rhyolite, mudstone which hosts stratiform mineralization, and basaltic sills and flows which are intercalated with turbiditic mudstones. The sequence

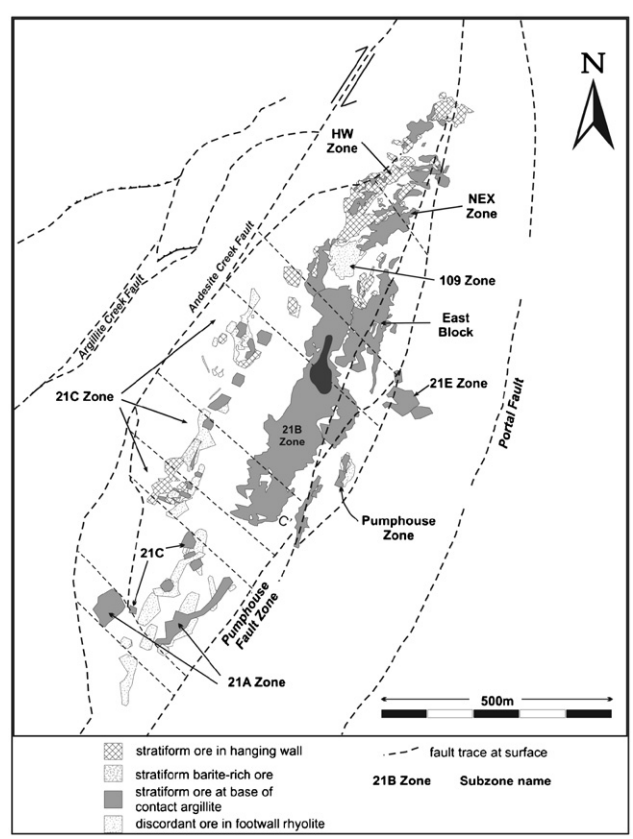

Fig. 1. Plan view of ore models in the Eskay Creek ♯21 Zone. Approximate extents of high-Hg area in the 21B zone is shown in dark shading.

is capped by a thick accumulation of clastic rocks, which fill the Bowser Basin. The metamorphic grade in the area is lower greenschist facies.

The Eskay Creek deposit is a polymetallic, gold and silver-rich, volcanic-hosted, massive sulfide deposit. By 2002, the mine had produced 2.25 million ounces of gold and 104.7 million ounces silver. The ore in the deposit is divided into subzones distinguished by mineralogy, texture, grade and metallurgical characteristics. The bulk of the stratiform ore is contained in the 21B and NEX zones, which are hosted by marine mudstone overlying rhyolite. Zone 21B is a tabular body of bedded sulfides and sulphosalts dominated by sphalerite, tetrahedrite and lead-sulphosalts with lesser galena and pyrite, and minor arsenopyrite. Stibnite and rarely cinnabar locally overprint the ore. Zone NEX lies north of the 21B lens, at the same stratigraphic horizon, and consists of mainly massive sphalerite, tetrahedrite, galena and lesser lead-sulphosalts, with late chalcopyrite stringers crosscutting the lens. The hanging wall (HW) zone is stratigraphically above the NEX zone, usually above the first basaltic sill, and is dominated by pyrite, sphalerite, galena and chalcopyrite. Stockwork vein and disseminated sulfides are present in the rhyolite, most notably in the 109, 21C and Pumphouse zones. Detailed descriptions of the geology and the orebodies are found in Edmunds et al. (1994), Roth et al. (1999), and Roth (2002).

4. Mineralogy

The three samples investigated in this study were derived from a localized, Hg-enriched domain in the 21B zone (Fig. 1, dark shading on the map) of the polymetallic Eskay Creek deposit. They are referred to herein as "B_1", "B_2" and "B_3". The samples are mainly fine- to medium-grained (Fig. 2) and consist of sphalerite, tetrahedrite $(Cu_{7.8}Ag_{1.51})(Fe_{0.19}Zn_{0.59}Hg_{1.25})(Sb_{3.74}As_{0.19})S_{13}$, cinnabar (HgS), stibnite (Sb_2S_3), pyrite (FeS_2), bournonite ($PbCuSbS_3$), Sb–Pb–S–(Cu)–(Ag) sulphosalts including boulangerite ($Pb_5Sb_4S_{11}$) and zinckenite ($Pb_6Sb_{14}S_{27}$), chalcopyrite ($CuFeS_2$), gold and electrum, arsenopyrite (FeAsS), galena (PbS), Fe-oxides and non-opaque minerals (Grammatikopoulos and Roth, 2002; Grammatikopoulos et al., 2005).

Sphalerite in the ground samples forms intergrowths (90%) predominantly with stibnite, zinckenite, galena, pyrite and non-opaque minerals (Fig. 2a,b). It displays granular, and mottled textures, but also occurs as free particles (<10%) and scarce inclusions (<1%) in other sulfides and sulfosalts. It is also the host of abundant pyrite, galena, tetrahedrite, chalcopyrite (locally disease-like) and gold inclusions.

The major carriers of Hg are cinnabar, sphalerite and tetrahedrite, and an array of complex Sb–Pb–S–(Cu)–(Ag) sulphosalts. Approximately, ~25–38% of the total Hg content is contained by sphalerite, 37–50% by cinnabar and 10–22% in tetrahedrite. The remainder of the minerals account for 3–11.5% of the total Hg content (Grammatikopoulos and Roth, 2002).

5. Chemistry of sphalerite

Sphalerite can incorporate a diverse suite of chemical elements in its structure. Fe, Cd and Cu commonly substitute for Zn in sphalerite, whereas Pb, In, Ga, Ge, Hg, Sn and Mn occur more sporadically (e.g. Oen et al., 1980; Viets et al., 1992; Ueno et al., 1996; Beaudoin, 2000; Di Benedetto et al., 2005). A total of 86 electron micro probe analyses were carried out on sphalerite in the present study. Most of the analyses were carried out in sample "B_3" because it contains most of sphalerite by volume %. Concentrations of nine elements (S, Zn, Hg, Fe, Cu, Mn, Sb, Ag and Pb) were determined at each point. However, values for Cu, Sb, Ag and Pb were below detection limits or very low. The average, minimum and maximum values of all the analyses are given in Table 2, and representative analyses in Tables 3–5. Compositional variations are shown in Figs. 3 and 4.

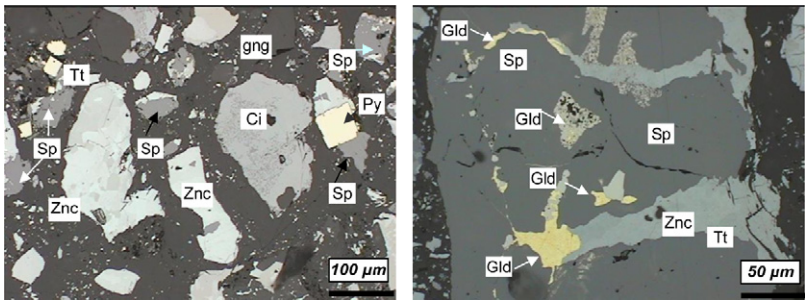

Fig. 2. Sample B_3. Pphotomicrographs in polarized reflected light: (a) Various free grains and intergrowths of cinnabar (Ci), tetrahedrite (Tt) and zinckenite (Znc), sphalerite (Sp), pyrite (Py), gangue minerals (gng). (b) Sphalerite that hosts intergrowths of tetrahedrite and zinckenite, and gold.

The data indicate the compositional inhomogeneity of Zn, Hg (and Fe) in sphalerite crystals. The Zn content in "B_1" ranges from 64.05 to 66.35 wt% and averages 64.66 wt%; in "B_2" from 61.67 to 66.15 wt% and averages 64.56 wt%; and in "B_3" from 52.82 to 66.47 wt% and averages 60.25 wt% (Table 2). The Hg content in "B_1" varies between 0.32 and 0.83 wt% and averages 0.63 wt%; in "B_2" between 0.08 and 6.56 wt% and averages 2.46 wt%; and in "B_3" between 0.48 and 16.35 wt% and averages 8.05 wt% (Table 2). The Fe content in "B_1" ranges from 1.15 to 2.29 wt% and averages 1.58 wt%, in "B_2" from 0.41 to 1.21 wt% and averages 0.82 wt%, and in "B_3" from 0.33 to 0.64 wt% and averages 0.47 wt% (Table 2). Subtle zoning in a few sphalerite grains identified with X-ray mapping reveals more information (e.g. Di Benedetto et al., 2005), but needs further refinement and will not be dealt herein.

Table 2. Average, minimum and maximum variations (wt%) of Zn, Hg and Fe in sphalerite from the three samples

	"B_1"	"B_2"	"B_3"
Zn			
Min	64.05	61.67	52.82
Max	66.35	66.16	66.47
Ave.	64.66	64.56	60.25
Hg			
Min	0.32	0.08	0.48
Max	0.83	6.56	16.35
Ave.	0.63	2.46	8.05
Fe			
Min	1.15	0.41	0.33
Max	2.29	1.21	0.64
Ave.	1.58	0.82	0.47

A frequency distribution diagram (Fig. 3a) shows that two different types of sphalerite can be distinguished based on the Hg contents; one with <0.04 atoms per formula unit (apfu) and one with >0.04 (apfu). The Hg content in "B_1" is dominated by class "1–2" (93%) and less (7%) by class "2–3". Hg content in "B_2" falls mainly in the ">0–1" class (61%), followed by 9% in the "1–2%" and 30% combined in the "5–6" and "6–7" classes. In "B_3" the distribution of Hg is largely bimodal, with classes of <3% Hg representing ca. 41%, and those with more than 8 wt% Hg, ca. 59%, while there is a noticeable gap between classes "3–4" to "7–8". Approximately, 58% of all analyses of Hg in sphalerite fall in the first three classes ("<0–3" combined).

A frequency distribution diagram (Fig. 3b) shows that the Fe content in "B_1" falls mainly in class "0.5–1" (71%) and less (29%) in ">0–0.5", whereas none is reported in class of "1–1.5". Fe content in "B_2" falls mainly in the "0.5–1" class (48%), followed by 39% in the "1–1.5" class and 13% in the ">0–0.5" class. In "B_3" the distribution of Fe is bimodal, similarly to "B_2", but the majority (65%) of the analyses fall in the ">0–0.5" and 35% in the "0.5–1" class. Approximately, 90% of all Fe analyses in sphalerite falls in the <1% class.

Table 3. Representative electron micro probe analyses and atomic proportions of sphalerite from "B_1"

Wt%	1	2	3	4	5	6	7	8	9	10
S	32.98	33.39	32.85	33.42	33.49	33.00	33.11	33.21	33.31	29.81
Fe	0.83	0.49	0.44	0.57	0.32	0.75	0.71	0.58	0.78	0.40
Cu	0.11	0.01	0.00	0.01	0.23	0.11	0.01	0.02	0.11	0.72
Pb	0.00	0.08	0.09	0.06	0.19	0.12	0.17	0.65	0.07	0.46
Sb	0.00	0.01	0.00	0.00	0.08	0.00	0.00	0.00	0.00	0.47
Zn	64.43	65.33	65.04	64.83	64.31	64.28	64.43	64.59	64.05	66.35
Ag	0.03	0.01	0.01	0.00	0.08	0.03	0.00	0.00	0.00	0.43
Mn	0.00	0.00	0.00	0.00	0.00	0.00	0.00	0.00	0.00	0.00
Hg	1.15	1.19	1.22	1.43	1.56	1.64	1.73	1.83	1.93	2.29
Total	99.53	100.51	99.65	100.32	100.26	99.93	100.16	100.88	100.25	100.93
At. Prop.										
Fe	0.015	0.009	0.008	0.010	0.006	0.013	0.013	0.010	0.014	0.007
Cu	0.002	0.000	0.000	0.000	0.004	0.002	0.000	0.000	0.002	0.011
Pb	0.000	0.000	0.000	0.000	0.001	0.001	0.001	0.003	0.000	0.002
Sb	0.000	0.000	0.000	0.000	0.001	0.000	0.000	0.000	0.000	0.004
Zn	0.990	0.994	0.998	0.988	0.981	0.984	0.984	0.979	0.977	1.005
Ag	0.000	0.000	0.000	0.000	0.001	0.000	0.000	0.000	0.000	0.004
Mn	0.000	0.000	0.000	0.000	0.000	0.000	0.000	0.000	0.000	0.000
Hg	0.006	0.006	0.006	0.007	0.008	0.008	0.009	0.009	0.010	0.011

Table 4. Representative electron micro probe analyses and atomic proportions of sphalerite from "B_2"

Wt%	1	2	3	4	5	6	7	8	9	10
S	33.34	33.02	32.80	32.90	32.95	32.57	30.85	31.04	30.90	30.86
Fe	0.41	0.77	1.21	1.15	1.04	0.45	0.63	0.54	0.49	0.60
Cu	0.00	0.28	0.02	0.00	0.03	0.22	0.41	0.09	0.18	0.00
Pb	0.00	0.00	0.43	0.00	0.00	0.22	0.16	0.00	0.08	0.02
Sb	0.00	0.00	0.00	0.00	0.01	0.49	0.12	0.02	0.03	0.04
Zn	66.16	65.36	65.10	65.61	65.56	65.32	62.38	62.15	62.05	61.88
Ag	0.00	0.07	0.00	0.00	0.00	0.11	0.07	0.02	0.00	0.00
Mn	0.00	0.00	0.00	0.00	0.00	0.10	0.37	0.40	0.36	0.56
Hg	0.08	0.11	0.88	0.92	0.94	1.04	5.63	5.75	5.93	6.56
Total	99.98	99.60	100.44	100.58	100.53	100.52	100.62	100.01	100.03	100.53
At. Prop.										
Fe	0.007	0.014	0.022	0.020	0.019	0.008	0.011	0.010	0.009	0.011
Cu	0.000	0.004	0.000	0.000	0.000	0.003	0.006	0.001	0.003	0.000
Pb	0.000	0.000	0.002	0.000	0.000	0.001	0.001	0.000	0.000	0.000
Sb	0.000	0.000	0.000	0.000	0.000	0.004	0.001	0.000	0.000	0.000
Zn	1.012	1.004	0.991	0.998	0.997	0.994	0.948	0.950	0.949	0.941
Ag	0.000	0.001	0.000	0.000	0.000	0.001	0.001	0.000	0.000	0.000
Mn	0.000	0.000	0.000	0.000	0.000	0.002	0.007	0.007	0.007	0.010
Hg	0.000	0.001	0.004	0.005	0.005	0.005	0.028	0.029	0.030	0.033

A plot of Zn versus the total content of divalent cations Fe + Mn + Hg illustrates a linear correlation ($R^2 = 0.9755$), as the Zn content decreases with increasing the sum of these cations (Fig. 4a). This relation indicates that significant contribution from other elements has not been neglected (e.g. Di Benedetto et al., 2005).

The data reveal that sphalerite shows an extensive incorporation of mercury, but limited substitution by Fe. A general negative relationship between Hg and Zn ($R^2 = 0.9985$) is evident (Fig. 4b). The very good linear correlation between the two elements excludes the possibility of cinnabar dispersion in sphalerite crystals.

Fe and Zn (Fig. 4c), Fe and Hg (Fig. 4d) and Mn and Hg do not show good correlations suggesting that substitution in sphalerite is dominated by the Hg–Zn pair of metals. However, these diagrams are useful because they display that the composite samples are composed of various sub-groups of sphalerite that may be directly related to various sub-samples used to make the three samples. Therefore, for geological and metallurgical purposes a better documentation of the various ore types may be required.

The overall bulk analyses of Hg in the samples ("B_3" = 54900 g/t, "B_2" = 1630 g/t and "B_1" = 1950 g/t) are in agreement with the variable Hg concentrations in sphalerite. Thus, it is not clear if the low Hg contents in sphalerite are dictated by mineral chemistry or the overall geochemistry of the samples, or this relationship is an artifact due to the limited number of analyses.

6. Discussion

Sphalerite is the dominant Zn-bearing phase and is distributed throughout the entire Eskay Creek deposit. EMPA of sphalerite of three composite samples revealed Hg-rich concentrations. The mineral conforms to the average formula $(Zn_{0.89-0.98}Hg_{0.01-0.09}Fe_{0.005-0.02})S$. Elemental variations are characterized by almost perfect substitution between Hg and Zn. The chemistry of the sphalerite is important for metallogenetic (e.g., Cook, 1996) but also metallurgical purposes.

Sphalerite has been described as the most refractory sulfide, potentially recording evidence for the conditions of its genesis (e.g., Craig and Vaughan, 1994; Cook, 1996). The examined samples are not single but composite, and consequently limit complete spatial analysis within this particular part of the ore body. However, considerable variability is displayed among the samples and within individual sphalerite grains (Fig. 4b,c). The data may suggest local variations that are related to precipitation process and chemistry of mineralizing fluids of the Eskay Creek deposit (Grammatikopoulos and Roth, 2002), as was already suggested in other studies (e.g. Craig and Vaughan, 1994; Cook, 1996; Di Benedetto et al., 2005; Tucker et al., 2005).

Small-scale variations result when a mineral grows from more or less evolved fluids at different times. Di Benedetto et al. (2005), for example, suggested that compositional variations in banded sphalerite crystals reflect physico-chemical variations that took place during crystal growth, rather than post-depositional

Table 5. Representative electron micro probe analyses and atomic proportions of sphalerite from "B_3"

Wt%	1	2	3	4	5	6	7	8	9	10
S	32.12	32.35	32.54	32.51	32.51	32.02	32.24	32.41	32.26	30.77
Fe	0.59	0.41	0.58	0.52	0.45	0.51	0.44	0.35	0.46	0.33
Cu	0.01	0.03	0.02	0.02	0.00	0.26	0.07	0.01	0.00	0.02
Pb	0.09	0.18	0.16	0.00	0.14	0.18	0.03	0.13	0.07	0.16
Sb	0.04	0.03	0.02	0.00	0.01	0.20	0.00	0.05	0.02	0.02
Zn	65.24	66.27	65.51	65.29	65.47	65.21	64.98	65.02	65.07	59.89
Ag	0.00	0.01	0.06	0.00	0.00	0.04	0.03	0.02	0.00	0.00
Mn	0.60	0.45	0.47	0.51	0.34	0.35	0.34	0.37	0.50	0.53
Hg	0.68	1.58	1.73	1.95	2.08	2.21	2.45	2.49	2.51	8.20
Total	99.37	101.30	101.08	100.81	101.00	100.99	100.57	100.84	100.89	99.91
At. Prop.										
Fe	0.011	0.007	0.010	0.009	0.008	0.009	0.008	0.006	0.008	0.006
Cu	0.000	0.000	0.000	0.000	0.000	0.004	0.001	0.000	0.000	0.000
Pb	0.000	0.001	0.001	0.000	0.001	0.001	0.000	0.001	0.000	0.001
Sb	0.000	0.000	0.000	0.000	0.000	0.002	0.000	0.000	0.000	0.000
Zn	1.004	0.998	0.989	0.990	0.989	0.988	0.988	0.986	0.986	0.917
Ag	0.000	0.000	0.001	0.000	0.000	0.000	0.000	0.000	0.000	0.000
Mn	0.011	0.008	0.008	0.009	0.006	0.006	0.006	0.007	0.009	0.010
Hg	0.003	0.008	0.009	0.010	0.010	0.011	0.012	0.012	0.012	0.041

Wt%	11	12	13	14	15	16	17	18	19	20
S	31.05	30.91	30.71	30.77	30.28	30.02	30.13	29.96	29.54	29.38
Fe	0.43	0.62	0.42	0.42	0.40	0.48	0.51	0.63	0.48	0.44
Cu	0.00	0.00	0.00	0.00	0.01	0.02	0.01	0.01	0.04	0.00
Pb	0.24	0.00	0.02	0.12	0.06	0.01	0.00	0.07	0.00	0.00
Sb	0.01	0.00	0.00	0.00	0.01	0.00	0.00	0.01	0.02	0.02
Zn	59.35	58.94	58.74	57.77	56.41	55.38	54.46	54.19	54.19	52.82
Ag	0.05	0.00	0.02	0.01	0.00	0.00	0.01	0.00	0.00	0.00
Mn	0.56	0.64	0.34	0.46	0.74	0.58	0.58	0.63	0.61	0.57
Hg	8.66	9.40	10.20	11.20	12.32	13.72	13.91	14.81	15.02	16.35
Total	100.34	100.51	100.45	100.76	100.23	100.21	99.62	100.32	99.91	99.57
At. Prop.										
Fe	0.008	0.011	0.007	0.008	0.007	0.009	0.009	0.011	0.009	0.008
Cu	0.000	0.000	0.000	0.000	0.000	0.000	0.000	0.000	0.001	0.000
Pb	0.001	0.000	0.000	0.001	0.000	0.000	0.000	0.000	0.000	0.000
Sb	0.000	0.000	0.000	0.000	0.000	0.000	0.000	0.000	0.000	0.000
Zn	0.905	0.897	0.894	0.877	0.861	0.845	0.836	0.826	0.829	0.811
Ag	0.000	0.000	0.000	0.000	0.000	0.000	0.000	0.000	0.000	0.000
Mn	0.010	0.012	0.006	0.008	0.013	0.011	0.011	0.012	0.011	0.010
Hg	0.043	0.047	0.051	0.055	0.061	0.068	0.070	0.074	0.075	0.082

re-equilibration processes. Further, in this study, mixing of different fluids (sea-water dominant hydrothermal fluid may have been modified by magmatic fluids; Sherlock et al., 1999) may have been important in controlling the chemistry of the sphalerite.

Determination of the compositional variation of the sphalerite in the deposit has also metallurgical implications because the mineral is mined for Zn. Any process aiming at separation and removal of mercury cannot be only physical in nature (flotation, gravity) because only 50% of the Hg occurs as cinnabar that can be physically removed (Grammatikopoulos and Roth, 2002). Mercury is a problematic impurity in zinc concentrates. It evaporates upon roasting and much of it ends up in the sulphuric acid produced from the roaster off-gases. However, because an important portion of the volatilized mercury ends up in the sulphuric acid, it decreases significantly the value of a by-product (Filippou D., pers. commun., 2005). Thus, the zinc refineries charge penalties for high mercury concentrates. If the distribution of mercury (e.g., in different ore types, or delineated zoning) is known in advance, the feed and/or the

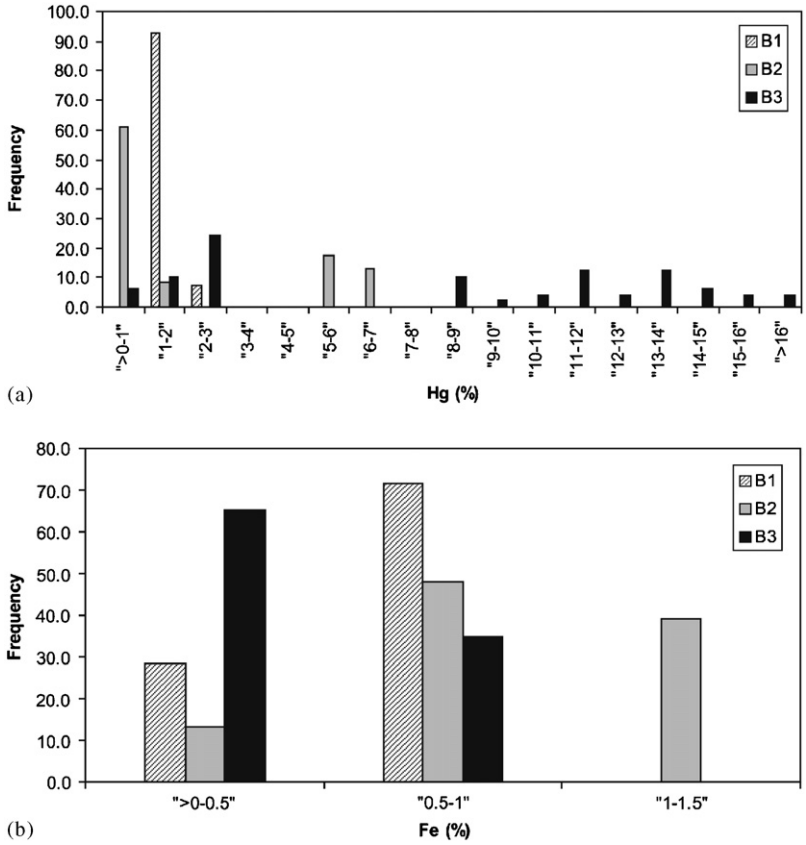

Fig. 3. Frequency distribution diagrams for (a) Fe and (b) Hg, respectively, from electron micro probe analyses of sphalerite.

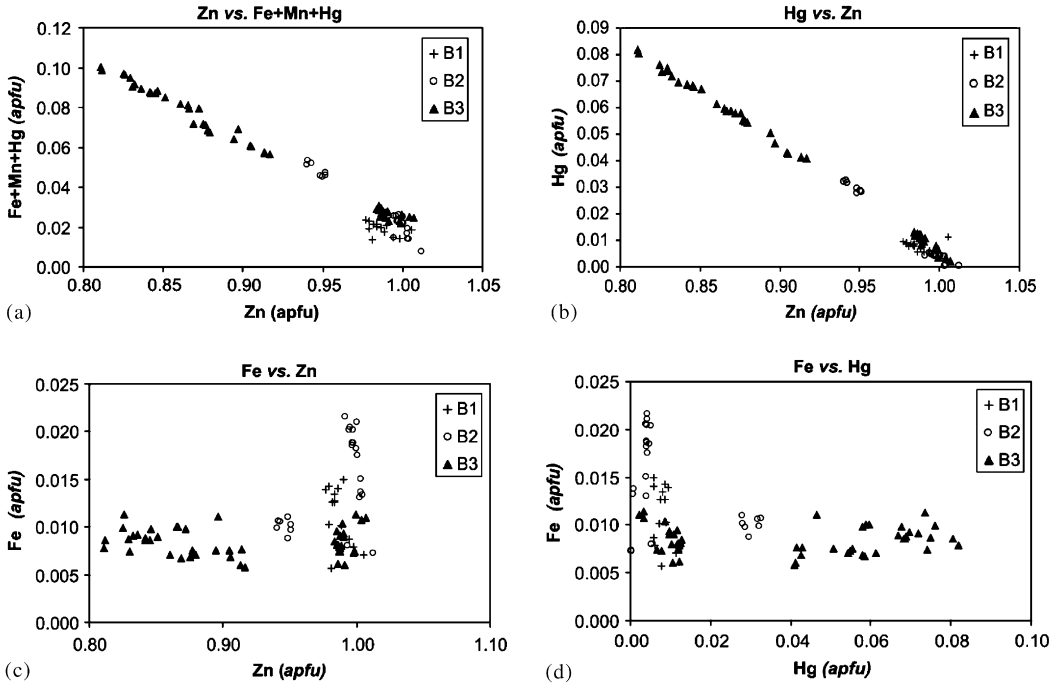

Fig. 4. Correlations between (a) Hg vs. Fe + Mn + Zn, (b) Fe vs. Zn, (c) Fe vs. Zn, (d) Fe vs. Hg of sphalerite from the three samples from the Eskay Creek deposit (apfu: atoms per formula unit).

concentrates can be blended from different mine zones, to avoid potential penalties. The Zn, Hg and Fe contents can be approximately estimated in the feed and final products of Zn depending on the proportions of the samples to be blended and processed.

7. Conclusions

The paper presents information on sphalerite that displays some unique chemical characteristics and is characterized by extensive incorporation of mercury. The data from the three samples suggest a possible compositional continuum within a localized, high-Hg domain of the Eskay Creek deposit. Overall, the Hg content in sphalerite ranges from ca. 0.08 to 16.35 wt%, while the highest Hg values are recorded in Fe-poor sphalerite. The predominant substitution in the mineral is that of the Hg–Zn pair.

The compositional differences among the three samples, but also in single composite samples, e.g. "B_3" (0.48–16.35 wt% Hg) may represent a temporal succession. However, the bimodality may be generated from comparing samples from different geometric types of ore or style of mineralization.

The data have the potential to be used for mapping fluid pathways for the deposit, and for metallurgical processing which may adjust and/or predict Zn recovery.

Acknowledgments

The author would like to thank Barrick Gold Corporation and SGS Lakefield Research for permission to use and publish part of the data. We are thankful to Prof. Dr. Udo Haack whose comments helped in improving the content of this manuscript, and also Dr. Dimitris Filippou for his comments on metallurgy of Hg.

References

Beaudoin, G., 2000. Acicular sphalerite enriched in Ag, Sb, and Cu embedded within color-banded sphalerite from the Kokanee Range, British Columbia, Canada. Can. Mineral. 38, 1387–1398.

Cook, N.J., 1996. Mineralogy of the sulphide deposits at Sulitjelma, northern Norway. Ore Geol. Rev. 11, 303–338.

Craig, J.R., Vaughan, D.J., 1994. Ore Microscopy and Ore Petrography. Wiley, New York 434pp.

Di Benedetto, F., Bernardini, G.P., Costagliola, P., Plant, D., Vaughan, D.J., 2005. Compositional zoning in sphalerite crystals. Am. Mineral. 90, 1384–1392.

Edmunds, F.C., Kuran, D.L., Rye, K.A., 1994. The geology of the 21 Zone deposits at Eskay Creek northwestern British Columbia, Canada. In: Black Hills Fifth Western Regional Conference on Precious Metals, Coal and the Environment, pp. 154–175.

Grammatikopoulos, T.A., Roth, T., 2002. Mineralogical characterization and Hg deportment in field samples from the Polymetallic Eskay Creek Deposit, British Columbia, Canada. Int. J. Surf. Min. Recl. 16, 180–195.

Grammatikopoulos, T.A., Roth, T., Valeyev, O., 2005. Compositional variation in Hg–Ag-rich tetrahedrite from the polymetallic Eskay Creek Deposit, British Columbia, Canada. N. Jb. Mineral. 181, 281–292.

Oen, I.S., Kager, P., Kieft, C., 1980. Oscillatory zoning of a discontinuous solid-solution series: sphalerite-stannite. Am. Mineral. 16, 1180–1195.

Roth, T., 2002. Physical and chemical constraints on mineralization in the Eskay Creek deposit, Northwestern British Columbia: Evidence from petrography, mineral chemistry, and sulfur isotopes. Unpublished Ph.D. Thesis, The University of British Columbia, 401pp.

Roth, T., Thompson, J.F.H., Barrett, T.J., 1999. The precious metal-rich Eskay Creek deposit, Northwestern British Columbia. In Volcanic-Associated Massive Sulfide Deposits. In: Barrie, C.T. Hannington, M.D. (Eds.), Volcanic-Associated Massive Sulfide Systems: Processes and Examples in Modern and Ancient Settings. Reviews in Economic Geology, vol. 8. pp. 357–373.

Sherlock, R.L., Roth, T., Spooner, E.T.C., Bray, C.J., 1999. Origin of the Eskay Creek precious metal-rich volcanogenic massive sulfide deposit: Fluid inclusion and stable isotope evidence. Econ. Geol. 94, 803–824.

Tucker, C.B., Taylor, C., Ames, D.E., 2005. Geology and metal contents of the Ruttan volcanogenic massive sulfide deposit, northern Manitoba, Canada. Mineral. Dep. 39, 795–812.

Ueno, T., Scott, S.D., Kojima, S., 1996. Inversion between sphalerite- and wurtzite-type structures in the system Zn–Fe–Ga–S. Can. Mineral. 34, 949–958.

Viets, J.G., Hopkins, R.T., Miller, B.M., 1992. Variations in minor and trace metals in sphalerite from Mississippi Valley-type deposits of the Ozark region: genetic implications. Econ. Geol. 87, 1897–1905.